Catalysis Today xxx (xxxx) xxx

Contents lists available at ScienceDirect

Catalysis Today

journal homepage: www.elsevier.com/locate/cattod

The determining role of T_x species in the catalytic potential of MXenes: Water adsorption and dissociation on Mo_2CT_x

José D. Gouveia *, José R.B. Gomes *

CICECO – Aveiro Institute of Materials, Department of Chemistry, University of Aveiro, Campus Universitário de Santiago, Aveiro, Portugal

ARTICLE INFO

Keywords:
Water gas shift reaction
2D materials
Carbides
Density functional theory
Periodic models

ABSTRACT

Density functional theory is used to investigate the origins of the excellent catalytic activity of the Mo_2CT_x MXene for the water gas shift reaction. By considering different possibilities for the MXene surface termination (T_x = none, O, F, or a mixture of O and F), we conclude that its ideal composition should contain both F and O adatoms, essential for controlling the exothermicity of the reaction and avoiding saturation by oxygenated species. More precisely, while Mo_2CO_2 and Mo_2CF_2 are too inert towards water adsorption and dissociation and the bare Mo_2C MXene is inactivated upon coverage by oxygenated species, our calculations predict that regions near one or two O adatoms in the midst of F surface terminations should be the active catalytic sites. Indeed, in the vicinity of the O adatoms, water adsorbs with moderate strength, dissociates with a very low energy barrier (0.14–0.20 eV), and the dissociation is moderately exothermic.

1. Introduction

To combat global warming and consequent climate changes, there is an urgent need for nearly carbon-neutral forms of energy production and storage. Hydrogen (H_2) is a promising energy carrier, expected to play a dominant role in energy systems soon. Around 70 Mtons of hydrogen are produced every year, but we are likely to start producing twice as much in the next 5 years [1]. Today, most of the hydrogen production derives from the steam methane reforming (grey hydrogen), using water and natural gas as reactants [2]. Aside from H_2, this process produces carbon monoxide (CO) which, through the water gas shift reaction (WGSR), becomes carbon dioxide (CO_2) and releases additional H_2. The H_2 resulting from these two reactions is used as fuel, while CO_2 can react with methane and be converted back into CO. This reaction is known as dry reforming, it consumes two greenhouse gases (methane and carbon dioxide) and yields CO and even more H_2. Alternatively, CO_2 can simply be dissociated into CO [3], used in the chemical industry [4], or recycled via the natural plant respiration cycle to generate biomass, completing the carbon cycle. Many of these processes involve the reaction of water dissociation. For example, the WGSR is known to begin with water dissociation, its rate-limiting step [5,6]. To satisfy the increasing demands of hydrogen production, research in this field focuses on discovering more efficient, cleaner and cheaper catalysts.

MXenes are two-dimensional (2D) transition metal carbides, nitrides, and carbonitrides, introduced in 2011 [7–9]. Over 30 MXenes have been experimentally synthesized so far, and they display extraordinary stability and potential for catalysis and energy storage, among other applications [10–13]. Structurally, monometallic MXenes are made up of layers of atoms of an early transition metallic element (M), alternated with layers of carbon or nitrogen (X = C or N), with stoichiometry $M_{n+1}X_nT_x$. In their bare form, MXenes contain only the M and X elements, for a total of 2n+1 atomic layers, with the M atoms occupying the outermost ones. Depending on synthesis conditions, MXenes are in fact produced with an additional termination layer (T_x) deposited over the outer metallic layers. The most common terminations are OH, O, H, or F, especially when using the hydrofluoric acid (HF) synthesis procedure [7,14,15], but MXenes with other terminations (e.g., Cl, S, NH_2) were experimentally prepared and/or their stability computationally investigated [16–19]. On each layer, the atoms are arranged in a triangular lattice, and consecutive atomic layers are known to be able to stack in one of two ways (face-centred cubic i.e., ABC, and hexagonal close-packed i.e., ABA), the most stable one depending on the M and X elements and on the surface termination [20]. Thus, MXenes can be produced with a huge variety of combinations of the M and X elements, T terminations, and atomic layer alignments. It is this versatility that confers these materials such a wide range of potential applications.

Recently, a density functional theory (DFT) study on water dissociation catalysed by 18 bare MXenes, conducted by our group, showed

* Corresponding authors.
E-mail addresses: gouveia@ua.pt (J.D. Gouveia), jrgomes@ua.pt (J.R.B. Gomes).

https://doi.org/10.1016/j.cattod.2022.07.016
Received 27 May 2022; Received in revised form 13 July 2022; Accepted 22 July 2022
Available online 23 July 2022

that the reaction is almost spontaneous on many of them [21]. This is a strong hint that MXenes should be excellent catalysts for processes that involve water dissociation. However, although bare MXenes have been obtained [14,22], they are hard to maintain, as they are very oxophilic and easily become covered by O adatoms. In fact, bare MXenes are very reactive in general, not only towards oxygen, which causes most chemical substances to adsorb too strongly on their surfaces, deterring their application as sensors [23] or in other phenomena which require more moderate adsorption strength, such as catalysis. As a matter of fact, many small gaseous molecules, such as O_2, spontaneously dissociate as they adsorb on MXenes [24]. On the other hand, a single oxygen surface termination layer shields the metal layer of MXenes, drastically reducing their reactivity. This allows their use as sensors [23,25] or, on the rare occasions in which the utilized reagents can bind to the O layer and this is enough to change the reaction mechanism, as catalysts [26]. Not long ago, Deeva et al.[14] and Li et al.[27] experimentally carried out the WGSR on the Mo_2CT_x MXene and the MXene-based $Pt@Nb_2CT_x$, respectively, with T_x = O, F, OH, and discovered that both materials showed remarkable stability and catalytic activity under the WGSR conditions. In the particular case of catalysis involving Mo_2CT_x, the termination was found to contain mainly F adatoms, in an F/Mo ratio of 0.7, as is commonly observed on MXenes synthesised using HF, while the remaining surface termination was mostly O. The authors additionally found that O binds much more strongly to Mo_2C than F does, so that, if the temperature was too high (above 550 °C), the F adatoms were removed, leaving behind a reduced surface which quickly got covered by oxygen. This was found to considerably decrease the activity of Mo_2CT_x for the WGSR. They also prepared a highly reduced sample and found that it decomposes to the corresponding Mo oxide, i.e., the bare Mo_2C surface is not stable under WGSR operando conditions. Otherwise, the MXene was deemed as highly stable and catalytically active, with a selectivity over 99 % towards CO_2 and H_2. Thus, F terminations seem to assume an important role (i) in the stabilization of the MXene catalyst and (ii) in regulating the strength of the surface-adsorbate interactions.

Computational models have reached such a level of reliability that their predictions consistently provide accurate guidelines for experimentalists. This work is motivated by the ease with which MXenes can dissociate water [21], by the fact that water dissociation is the first and often rate-determining step of several reactions of industrial relevance that require breaking this molecule [5,6], and by the experimentally demonstrated catalytic activity of the Mo_2CT_x MXene towards the WGSR [14]. Here, we employ DFT calculations to analyse the mechanism of water adsorption and dissociation on the Mo_2CT_x MXene, separately considering four different surface terminations: the bare MXene, the surface fully covered by O or F, and the MXene terminated by a combination of F and O adatoms. Consequently, this study provides information about the effect of MXene surface terminations (T_x) on water adsorption and on the catalysis of the water dissociation reaction. This is the first step towards understanding the mechanism by which reactions such as WGS and steam reforming occur on the Mo_2CT_x MXene, and most likely on MXenes made of other M or X elements. In the following, we describe our computational procedure, present and discuss the results and, finally, summarize the conclusions.

2. Computational methods

All ab initio calculations were performed using the VASP package [28–31]. The exchange-correlation functional of choice was the one prescribed by Perdew-Burke-Ernzerhof (PBE) [32], including D3 dispersion corrections [33,34] to correctly describe the van der Waals interactions that govern adsorption phenomena on MXenes [3,20,21,23,25,35–38]. The wave function of valence electrons was expanded as plane waves using a basis set with an energy cut-off of 415 eV, while core electrons were implicitly considered using the projector augmented-wave (PAW) method [39]. The valence electron configurations considered for each element have been shown to yield accurate results for MXenes [3,20,21,37], and were as follows: H ($1s^1$), C ($2s^2$ $2p^2$), O ($2s^2$ $2p^4$), F ($2s^2$ $2p^5$), Mo ($4p^6$ $4d^5$ $5s^1$). Orbital occupations were set using Gaussian smearing with a width of 0.01. The total energies were converged within 10^{-7} eV and the atomic positions were relaxed until the forces acting on the atoms were all below 0.005 eV/Å. The Brillouin zone was sampled as a Γ-centred 3 × 3 × 1 grid of special **k**-points [40]. By conducting preliminary tests using stricter convergence criteria, k-point grids with higher density, and higher energy cut-offs, we can safely state that relative energies are converged within 3 meV. We additionally found that spin polarization has no effect on the results presented here.

Our goal is to calculate water adsorption energies (E_{ads}), and water dissociation activation barrier (E_b) and reaction (E_{reac}) energies. The reaction steps are shown in Fig. 1. Configurations corresponding to saddle points of the potential energy hypersurface, along the minimum-energy path for water dissociation, i.e., reaction transition states (TS), were found using the dimer method [41]. The activation energy for water dissociation was calculated as the difference between the total energy of the MXene+H_2O system in its TS and in its adsorbed state. Water adsorption energies were calculated as the difference between the total energy of the Mxene+H_2O system when water is adsorbed, and when the surface and the molecule are infinitely separated, i.e.,

$$E_{ads} = E(\mathrm{MXene} + H_2O) - [E(\mathrm{MXene}) + E(H_2O)], \quad (1)$$

where E(x) is the total energy of a supercell containing x. The configuration of the system after water dissociation was found by calculating the normal modes of vibration of the system in its TS configuration, within the harmonic approximation via diagonalization of the Hessian matrix with elements computed as finite differences of 0.015 Å of analytical gradients. The frequencies calculated in this way were also used to calculate the zero-point energy (ZPE) contribution to the total energy of all systems in this work. The normal vibrational mode of the TS corresponding to water dissociation can easily be identified since its vibrational frequency is imaginary, and it corresponds to an oscillation between adsorbed water in its molecular state and its dissociated (OH+H) state. The water dissociation reaction energy, as catalysed by Mo_2CT_x, was calculated as

$$E_{reac} = E(\mathrm{MXene} + \mathrm{OH} + \mathrm{H}) - E(\mathrm{MXene} + H_2O). \quad (2)$$

To model the Mo_2CT_x MXene (0001) basal surface, a rhombic supercell was considered, containing a $p(4 \times 4)$ grid of Mo_2CT_x unit cells, accounting for a total of 80 or 48 atoms of Mo_2CT_x with or without surface terminations, respectively. Periodic boundary conditions were assumed in all cartesian directions, as shown in Fig. 2. To avoid unwanted interaction between periodic copies of the system in the direction perpendicular to the surface, the cell height was fixed to contain at least 15 Å of vacuum.

As can be seen in Fig. 2, an ABA atomic layer stacking was assumed for the Mo_2CT_x model with and without surface termination. The justification is manifold, and originates from previous theoretical and experimental results, as well as from results obtained in this work. The bare Mo_2C was the first Mo_2CT_x MXene to be shown to be thermodynamically more stable when adopting an ABA atomic layer stacking, rather than the traditional ABC one, by 0.24 eV per unit cell [42]. Later, we found that the addition of an O adatom surface terminating layer, yielding Mo_2CO_2, causes the material to prefer the ABA stacking by an even larger margin with respect to ABC, over 1.5 eV [20]. Most recently, we further predicted that, on Mo_2CF_2, ABA stacking is also the ground state, more stable than ABC by around 0.27 eV [43]. Deeva et al. synthesized the Mo_2CT_x MXene using the HF method to etch out the Ga atoms from the Mo_2Ga_2C MAX phase, and obtained an Mo_2CT_x MXene with hexagonal symmetry [14]. The cell parameter a of the resulting MXene was reported to be 2.8629 Å, down from 3.037 Å in the precursor Mo_2Ga_2C. This reduction is consistent with a transition from an ABC-aligned structure in the parent MAX phase, to a more stable ABA

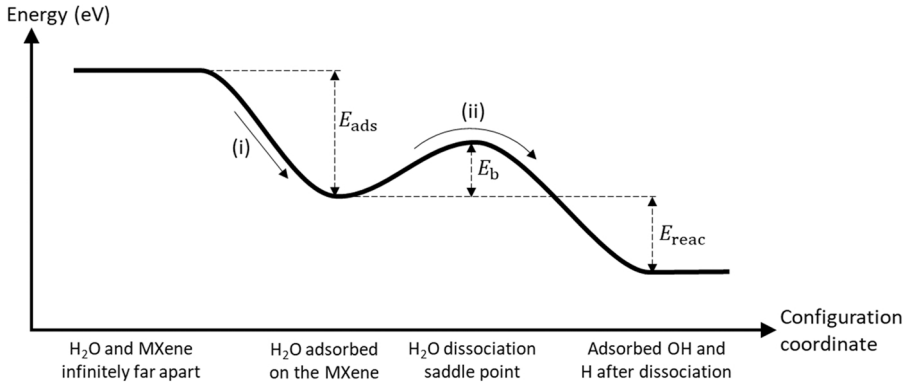

Fig. 1. Schematic energy profile for water dissociation on Mo_2CT_x. Step (i) corresponds to molecular adsorption, with adsorption energy E_{ads}, and step (ii) to dissociation into coadsorbed OH+H, with activation energy E_b and reaction energy E_{reac}.

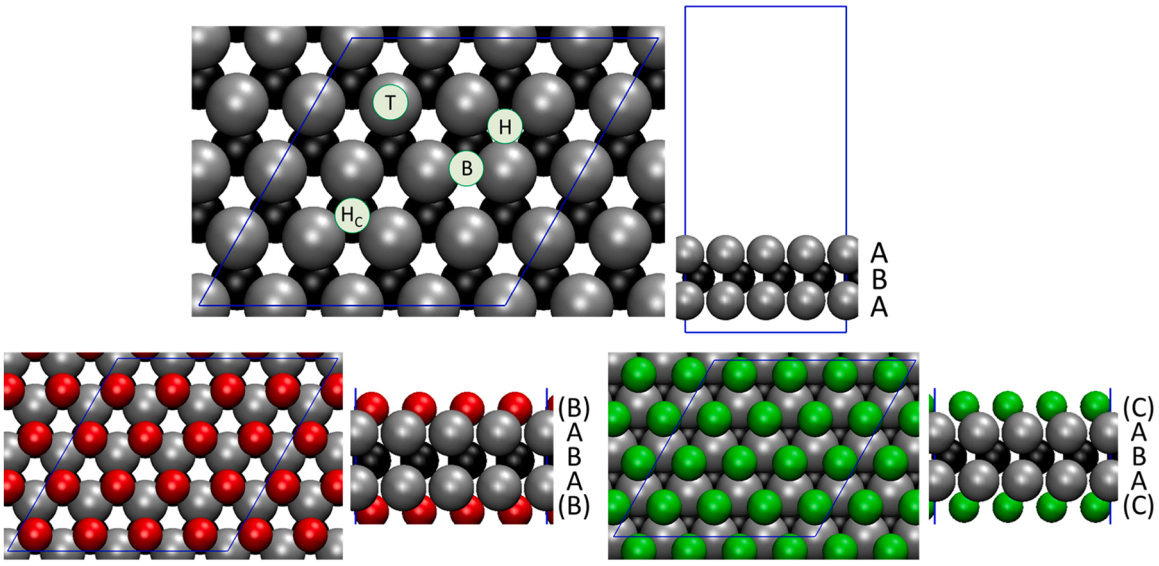

Fig. 2. Top and side views of the Mo_2CT_x MXene without any surface termination (top images), with oxygen termination (bottom left images), or with fluorine termination (bottom right images). On the top view of Mo_2C, letters inside circles are placed at high-symmetry sites on the surface: top (T), bridge (B), hollow (H), and hollow-C (H_C). The letters next to the side views refer to the relative alignment of the atomic layers of the surface, with the surface termination layers in parenthesis, and the blue lines delimit the supercell considered in the calculations. Colour code for spheres: C in black, O in red, Mo in grey, and F in green.

stacking of the synthesized MXene, as the latter is known to display a much smaller cell parameter a than the corresponding ABC-aligned MXene [20,42].

Table 1 shows the calculated lattice parameters of Mo_2CT_x, with different surface terminations and atomic layer stacking phases. Note that the PBE functional, as used in this work, provides very reliable results on this matter, often yielding lattice parameters within 1–3 % of experimental measurements, as seen, for example, in Refs. [44–46]. In the case of bare Mo_2C, the obtained value of a with ABC atomic layer stacking (2.99 Å) is closer to the one measured for the Mo_2Ga_2C MAX phase (≈3.04 Å) [14], while the one calculated for ABA-stacked Mo_2C (2.84 Å) is within less than 1 % of the value measured for the Mo_2CT_x MXene (2.86). While one would not expect the cell parameter calculated for an MXene surface to necessarily match the one of its parent MAX structure, the similarity between the a value of ABA Mo_2C and the one measured for Mo_2CT_x is remarkable. Qualitatively, the calculated cell parameter of Mo_2CO_2 match the measured ones in the same way as for Mo_2C. However, when compared to the measured MXene value of a, there is an even better match with the calculated ABA cell parameter, and an even worse match with the corresponding ABC value. The calculated cell parameter of ABC Mo_2CO_2 is not as close to the one measured for the MAX phase as that of ABC Mo_2C. Most likely, this is because the MAX phase contains the Mo_2C stoichiometry and structure, but no oxygen or fluorine, making it very different from Mo_2CT_x with any surface termination. Lastly, the calculated cell parameter for ABA Mo_2CF_2 differs by around 1 % from the one measured for Mo_2CT_x. The

Table 1
Cell parameter (a) of Mo_2CT_x, with different surface terminations (O, F or none) and atomic layer stacking phases (ABC or ABA). The second column shows the a values calculated in this work. The third and fourth columns are the relative percent difference between the calculated cell parameters and the ones measured by Deeva et al. [14] for the Mo_2Ga_2C MAX phase (3.037 Å) and for the Mo_2CT_x MXene (2.8629 Å), respectively. For example, the cell parameter a calculated for Mo_2CO_2 with ABA stacking (2.88 Å) differs from the one measured for the Mo_2CT_x MXene by 0.6%.

MXene	a (Å)	δa% (MAX)	δa% (MXene)
Mo_2C (ABC)	2.99	-1.5	4.4
Mo_2C (ABA)	2.84	-6.5	-0.8
Mo_2CO_2 (ABC)	3.10	2.1	8.3
Mo_2CO_2 (ABA)	2.88	-5.5	0.6
Mo_2CF_2 (ABC)	3.27	7.7	14.2
Mo_2CF_2 (ABA)	2.90	-4.5	1.3

surface of the Mo_2CT_x MXene synthesized in Ref. [14] contained F adatoms in an F/Mo ratio of 0.7, and the remaining surface termination was composed of O adatoms, so that, of all the stoichiometries present in Table 1, the one closest to the experimental one is Mo_2CF_2. According to the values in this Table, the *a* cell parameter of ABC-stacked Mo_2CF_2 is higher than the one measured in Ref. [14] for Mo_2CT_x by more than 14 %. Aside from the *a* lattice parameter, the distance between the two Mo layers measured in Ref. [14] (≈3 Å) is also significantly closer to the one displayed by our ABA-stacked Mo_2CT_x models (≈2.8 Å) than to the one we obtained for the ABC-stacked systems (≈2.3 Å). All the results presented in these two paragraphs are strong hints that the synthesised MXene exhibits ABA stacking, and therefore we can safely assume this stacking in our MXene models.

As seen in the side views of Mo_2CO_2 and Mo_2CF_2 in Fig. 2, the lattice site on which the O and F surface termination layers adsorb are distinct – a hollow-C (H_C) site for oxygen and a hollow (H) site for fluorine. Oxygen can also adsorb on a hollow site, but this alignment is metastable by more than 1 eV and easily transitions to the H_C ground state, with an activation energy below 0.2 eV. On the other hand, fluorine prefers an adsorption site that is staggered with respect to the carbon layer, as shown in Fig. 2, a configuration that is more stable than being directly aligned with the C layer by 0.3 eV. Besides bare and fully O- or F-terminated Mo_2CT_x models, we also considered a mix between O and F surface terminations, for a more realistic model of the MXene synthesized in Ref. [14], which contained both elements. The F termination was found to be a requirement to keep the MXene from oxidizing. Indeed, MXenes are extremely oxophilic and usually even adsorb molecular oxygen dissociatively, which makes O-terminated MXenes practically inert and unsuited for catalytic applications that require the binding of reactants to metallic atoms of MXenes [24]. If the F adatoms are removed, space left behind on the surface is quickly filled by oxygen. However, this does not imply that oxygen is only a nuisance and should be completely removed, as we show in the following sections. Since the surface termination of the as-synthesised and WGSR-active Mo_2CT_x MXene contained mostly F adatoms [14], our models of the mixed-termination surface were built from that of Mo_2CF_2, keeping its lattice parameter (which diverges from that of Mo_2CO_2 by less than 1 %). Then, we created two models, containing one or two oxygen atoms, replacing F ones. The O adatoms were added on their preferred adsorption site – vertically aligned with a C atom of the inner MXene layer, as shown in Fig. 3. Each O atom replaced more than one F atom due to lateral F-O repulsion, which would not allow all atoms to fit into the available unit cells. In particular, the O adatom of the one-O model replaced three F adatoms, while the two O adatoms of the two-O model replaced five F adatoms. The first of these models was developed to represent the simplest oxygen-containing patch of the Mo_2CF_2 surface. The second model was studied because, on its topmost atomic layer, it contains 11 F adatoms bonded to 16 Mo atoms, for an F-to-Mo ratio of 0.69, which is near the experimentally measured value of 0.7 [14]. The two-oxygen model can also be thought of as representing a region of the Mo_2CF_2 surface without T_x species where an oxygen molecule adsorbed and dissociated.

3. Results and discussion

3.1. Bare Mo_2C

The simplest MXene model studied in this work is that of the bare Mo_2C MXene surface (Fig. 2). This surface comprises three atomic layers – an inner C layer surrounded by two Mo layers – in a hexagonal close-packed configuration. The adsorption of a water molecule occurs on a top site of the Mo_2C surface (see the left images in Fig. 4). The molecule sits approximately parallel to the surface, at an Mo-O distance of 2.37 Å, which is an atomic arrangement analogous to the one found for ABC-stacked Mo_2C [21]. The adsorption configuration is symmetric with respect to the plane containing the C_2 axis of the water molecule and passing between the two hydrogen atoms. The calculated O-H bond lengths and H-O-H bond angle, of 0.98 Å and 105.8°, remain approximately the same as the ones obtained for gaseous water. The adsorption energy is − 0.62 eV, which is weaker by 0.3 eV than the corresponding value on ABC-stacked Mo_2C [21]. A very small amount of electric charge is transferred from the surface to the molecule, of ca. 0.03 *e*, where *e* is the charge of an electron.

The transition state of water dissociation consists of one of the hydrogens approaching the surface towards a hollow site, as shown in the central panels of Fig. 4, at a distance of 1.36 Å from the plane of Mo atoms, so that the distance between this hydrogen and the oxygen atom increases to 1.38 Å. The activation energy is 0.41 eV, a value that is 0.08 eV higher than the corresponding one on ABC-stacked Mo_2C [21]. The activation energy value is lower than the absolute value of the water adsorption energy, therefore, after adsorption, the molecule is more likely to dissociate than to desorb from the MXene. After dissociation, the resulting OH and H species are adsorbed at nearby hollow sites (right images of Fig. 4). According to our calculations, the dissociation reaction is more exothermic than on the ABC-stacked Mo_2C, by 0.4 eV, with a reaction energy of − 1.39 eV. The results in this paragraph hint that ABA-stacked Mo_2C should be a suitable catalyst for dissociating water, following the trend of all the bare ABC-stacked MXenes [21]. In a realistic environment, MXene patches without any surface termination might be rare, since they are easily covered by O adatoms, and the surface becomes inert for this reaction. However, if small patches spanning at least two unit cells are present, they can contribute to the catalytic activity for water dissociation.

3.2. Oxygen-terminated Mo_2C (Mo_2CO_2)

Bare MXene surfaces are very oxophilic [24] and ABA-stacked Mo_2C is no exception. Our calculations predict that, like its ABC counterpart, oxygen molecules adsorb dissociatively with adsorption energies around − 8 eV, implying that the removal of an oxygen adatom requires an

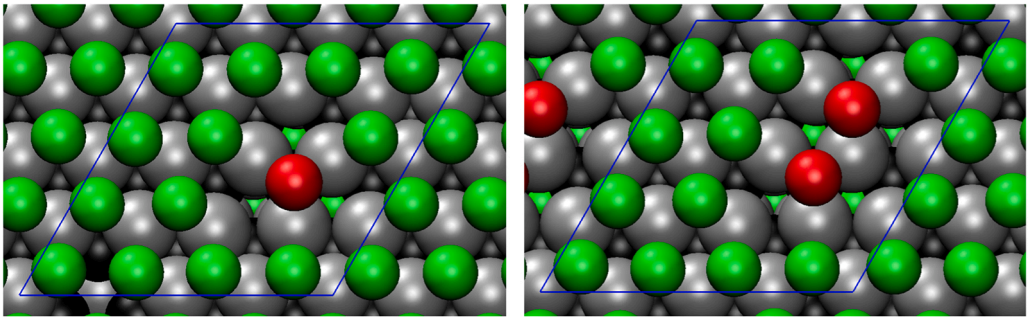

Fig. 3. Top view of our models of the Mo_2CT_x MXene with its surface terminated by F and one (left image) or two (right image) O adatoms. The blue lines delimit the supercell considered in the calculations. Colour code for spheres: C in black, O in red, Mo in grey, and F in green.

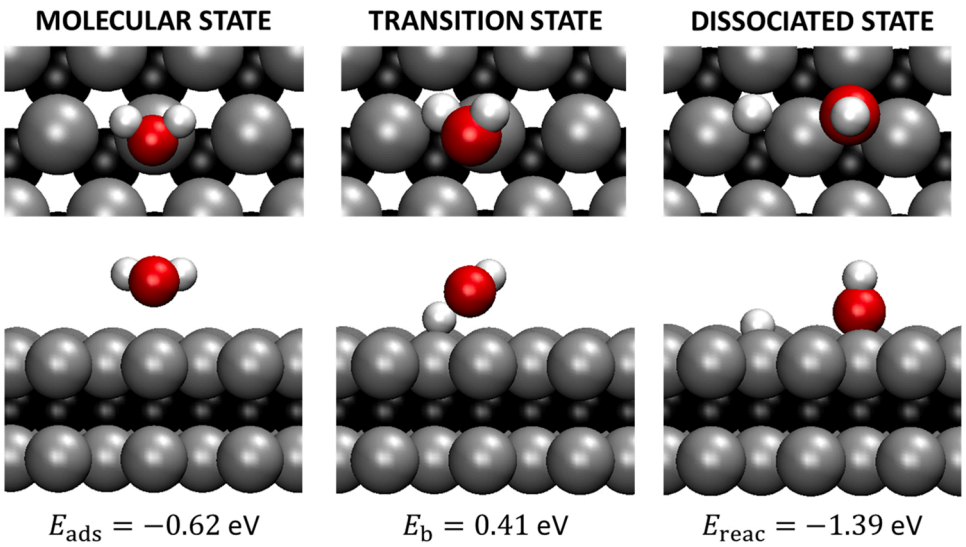

Fig. 4. Top (top images) and side (bottom images) views of the ground state configuration of a water molecule adsorbed on Mo_2C (left images), the saddle point configuration of water dissociation (centre images), and the dissociated configuration (right images). The adsorption energy (E_{ads}), activation energy (E_b), and reaction energy (E_{reac}) are shown below the system representations and compiled in Table S1. Colour code for spheres: C in black, O in red, Mo in grey, and H in white.

energy of roughly 4 eV [43]. For this reason, large areas of MXene surfaces are commonly covered by a layer of oxygen adatoms that originate from the environment. This layer serves as a shield for the metallic layers underneath and keeps most molecules from binding to them. We observed this effect upon simulation of the adsorption of a water molecule on the Mo_2CO_2 MXene, shown in the left images of Fig. 5.

The interaction takes place with the water molecule remaining perpendicular to the surface, with its two hydrogen atoms aimed at two surface oxygen adatoms, forming two weak hydrogen bonds with length 2.25 Å, for an adsorption energy of − 0.20 eV. The adsorption configuration is symmetric with respect to the plane containing the C_2 axis of the water molecule and passing between the two hydrogen atoms. The adsorption is considerably weaker on this surface than on bare Mo_2C and does not involve the formation of covalent bonds or any apparent interaction with Mo atoms of the surface – the distance between the water O and the closest Mo is just over 4 Å, while the Mo-O distance for surface O adatoms is 2 Å. Thus, it stands to reason that catalysis of water dissociation on this surface is energetically expensive, as this interaction is required to facilitate the reaction.

We found that the transition state configuration for water dissociation on Mo_2CO_2 is a late one, i.e., closer to the products of the reaction than to the reactant, as shown in the centre images of Fig. 5, and the activation energy is 2.50 eV, which is close to half as much as the O-H bond energy in a water molecule. For the molecule to reach this state, it must turn itself around to allow its oxygen atom to bind to an oxygen

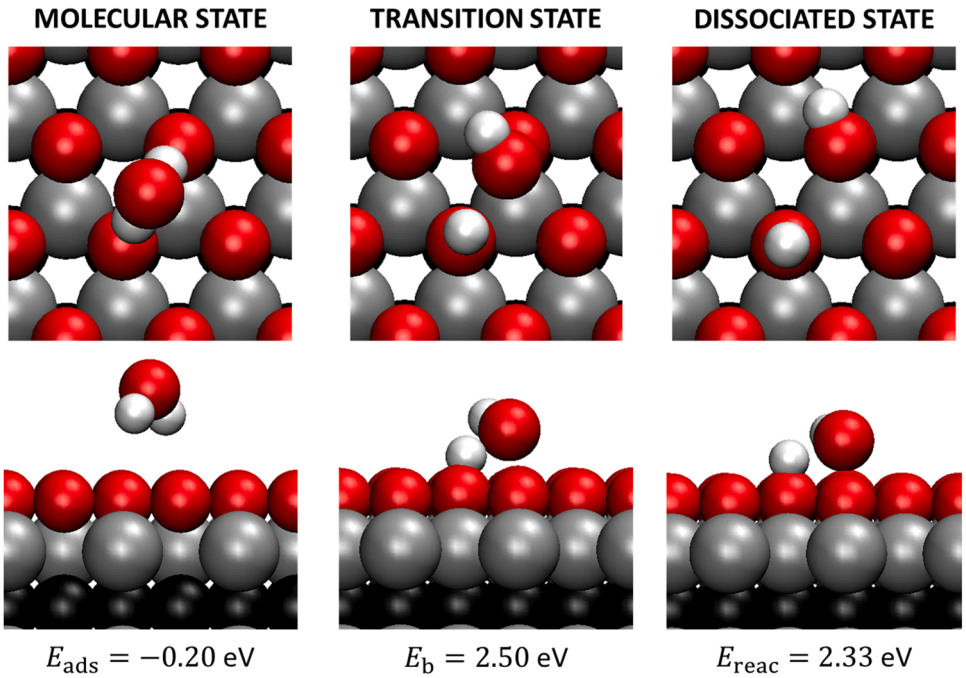

Fig. 5. Top (top images) and side (bottom images) views of the ground state configuration of a water molecule adsorbed on Mo_2CO_2 (left images), the saddle point configuration of water dissociation (centre images), and the dissociated configuration (right images). The adsorption energy (E_{ads}), activation energy (E_b), and reaction energy (E_{reac}) are shown below the system representations and compiled in Table S1. Colour code for spheres: C in black, O in red, Mo in grey, and H in white.

atom of the surface, while one of the O-H bond lengths increases to twice its initial value, to around 2.13 Å. After an endothermic dissociation, with a reaction energy of 2.33 eV, the OH species remains bound to an O adatom of the surface, locally forming an OOH (hydroperoxide) surface termination, and the released H atom binds to a neighbouring O adatom of the surface, locally forming a hydroxyl surface termination (see the right images of Fig. 5). Observation of the dissociated state shown in Fig. 5 suggests that one might be able to form H_2 via rotation of the OOH group towards OH. We investigated this possibility and found that it would involve a very high energy barrier around 3 eV. Alternatively, if one wished to conduct the WGSR, CO could adsorb near OOH and form OCOH, a surface intermediate suggested to play a central role in the WGSR on metallic surfaces [5,6]. In this case, we found that CO can indeed physisorb nearby and form a chemical bond with the central O of OOH. Instead of forming an OCOH adsorbate, a CO_2 molecule is spontaneously released, and the hydrogen atom bonds with a surface O to form another OH group. This process can be represented as the following sequence of reactions,

$$*OOH + CO \rightarrow *OOH + *CO, \quad (3)$$

$$*OOH + *CO \rightarrow *OH + *CO_2, \quad (4)$$

$$*OH + *CO_2 \rightarrow *OH + CO_2, \quad (5)$$

where *XY represents an XY species adsorbed through the X atom. Here, the first step is CO adsorption (Eq. 3), which occurs spontaneously with an E_{ads} of − 0.40 eV. The second step is CO_2 formation (Eq. 4), with a low activation energy, 0.32 eV, and high exothermicity, by − 4.10 eV. The last step in the sequence is CO_2 release (Eq. 5), with a desorption energy of 0.37 eV, which is much smaller than the energy (−1.62 eV) required to desorb CO_2 from the Mo_2C MXene surface. Note that, despite several attempts, because of the large exothermicity of the reaction described by Eq. 4, the formation of the OCOH intermediate was not possible.

As expected, we predicted the Mo_2CO_2 MXene surface to be unsuitable to catalyse the water dissociation reaction. The adsorption is too weak, the energy barrier is too high, and the reaction is very endothermic. All of these make it very unlikely that water dissociation takes place in areas of the MXene that are fully covered by a layer of oxygen, since the molecule is much more likely to desorb instead. Nevertheless, the most important detail to retain from this section is that, after dissociation occurs, all the products of the reaction remain bound to the surface and no atoms of the catalyst are removed, hence preserving its integrity.

3.3. Fluorine-terminated Mo_2C (Mo_2CF_2)

When an MXene is synthesised via the HF method, it often becomes covered by a layer composed mainly of F adatoms [7,14,15]. In this section, we investigate the mechanism of water dissociation in regions of the Mo_2CT_x MXene that are completely covered by F, i.e., on Mo_2CF_2. On this surface, we observed that water adsorption occurs in a configuration analogous to the one found for Mo_2CO_2, shown in the left images of Fig. 6. The adsorbate forms two weak hydrogen bonds with surface F adatoms, of length around 2.36 Å, and again there is no covalent water-MXene interaction since the Mo-O distance is higher than 4 Å. The adsorption energy is − 0.13 eV, making this the weakest adsorption here described so far, suggesting a hydrophobic character for the fluorine-terminated Mo_2C surface.

Unlike O adatoms on Mo_2C, which prefer adsorbing on H_C sites over hollow ones by more than 1 eV, F adatoms are not as demanding. They adsorb more weakly overall, on hollow sites, and the energetic difference between being placed on this site and on H_C or T sites is only 0.3 or 0.4 eV, respectively. This allows for a seemingly unexpectedly low-energy transition state (E_b = 0.31 eV) for water dissociation. In this state, the water molecule approaches the surface, on a B site, and its O atom becomes bound to the two adjacent Mo atoms (centre images of Fig. 6), with bonds of order around 0.42, calculated with the DDEC6 method [47], similar to the O-H bond orders of 0.67 and 0.32 present in the same configuration. The Mo-O bonds in the TS state have lengths around 2.20 Å, comparable to the estimated Mo-O bond lengths of 2.06 Å on Mo_2CO_2. Simultaneously, an F adatom is pushed away from its original hollow site onto a top site. One of the hydrogens bridges the O and F atoms, 1.27 Å and 1.06 Å away, respectively. If the H atom moves closer to the F atom on the T site, the water molecule dissociates and the system relaxes to a new minimum, as shown in the right images of Fig. 6. After exothermic dissociation, with reaction energy − 1.06 eV, the resulting OH group replaces the previously adsorbed F atom, and an HF molecule is released, forming two hydrogen bonds, [Mo]—OH•••FH•••F—[Mo]. Due to the oxophilicity of the Mo_2C MXene, this process effectively keeps the catalyst from regenerating, since OH binds to the surface (E_{ads} = − 1.29 eV) considerably more strongly than HF (E_{ads} = − 0.30 eV). Thus, dissociation of a water molecule on Mo_2CF_2 irreversibly inactivates the catalytic site because one F group is removed. In some sense, this is analogous to the experimental observation of Deeva et al. [14], according to which the partial removal of the F termination does not improve the reaction rates because the partially reduced Mo_2C surface rapidly becomes covered with oxygen. Moreover,

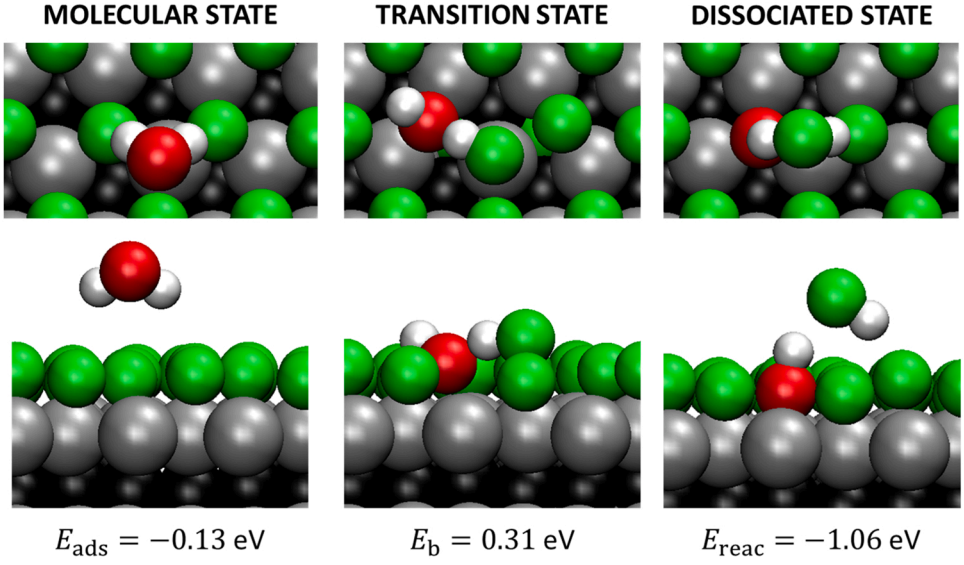

Fig. 6. Top (top images) and side (bottom images) views of the ground state configuration of a water molecule adsorbed on Mo_2CF_2 (left images), the saddle point configuration of water dissociation (centre images), and the dissociated configuration (right images). The adsorption energy (E_{ads}), activation energy (E_b), and reaction energy (E_{reac}) are shown below the system representations and compiled in Table S1. Colour code for spheres: C in black, O in red, F in green, Mo in grey, and H in white.

water dissociation in an F-terminated region of Mo_2CT_x is unlikely to occur because the energy barrier (0.31 eV) is higher than the absolute value of the adsorption energy (0.13 eV).

3.4. Fluorine- and oxygen-terminated Mo_2CT_x

The results presented in the previous sections reveal the role of the F and O terminations in tuning the behaviour of the Mo_2C MXene towards water adsorption and dissociation. The bare Mo_2C surface appears to be suited for these two phenomena, but it is also too reactive and can easily become saturated with all kinds of adsorbates, including the products of water dissociation themselves, hindering its regeneration as a catalyst. Mo_2CO_2 is more stable than the bare MXene, and therefore less reactive. This surface has the catalytic disadvantages of water adsorbing very weakly, and its dissociation requiring surpassing a high energy barrier, while the fact that the products of water dissociation remain adsorbed on the surface is a point in favour. Lastly, the F-covered surface (Mo_2CF_2) appears to be more flexible in terms of lateral motion of the terminating species, allowing water to bind with metal atoms of the MXene. In fact, despite the weak water molecule adsorption on Mo_2CF_2, a low activation energy for its dissociation was found because, in the TS configuration, water can form temporary covalent bonds with Mo atoms, which appears to be a requirement for lowering the dissociation energy barrier. However, after dissociation, an HF molecule is released, and an OH group remains adsorbed on the surface instead of the previously present F adatom, damaging the catalytic surface. Hence, the ideal region of an Mo_2CT_x surface for conducting water dissociation should combine the advantages of Mo_2C (water bonding to surface Mo atoms), Mo_2CO_2 (preservation of the integrity of the MXene after water dissociation), and Mo_2CF_2 (protection against oxidation and subsequent deactivation of the catalyst). Here, we show that this can be achieved by considering the Mo_2CT_x MXene locally terminated by O and F adatoms. We consider two models: one with a single O adatom, and another with two, as shown in Fig. 3. Since we employ a supercell with 16 MXene unit cells, the former would correspond to a rather dilute distribution of O, while the latter displays the experimentally measured F:Mo species ratio. In the following, we show that the vicinity of these O adatoms amidst the F surface termination should be a suitable active site for water adsorption and dissociation.

Let us first discuss the one-O Mo_2CT_x model. On this surface, a water molecule adsorbs by forming an Mo-O covalent bond (left images of Fig. 7), with bond order 0.33 and length 2.34 Å, complemented by an electron transfer of 0.08 *e* from the molecule to the MXene. Both O–H bonds retain their gas phase length value of 0.98 Å. One of the hydrogens is directed at the surface oxygen adatom, forming a hydrogen bond with length 1.82 Å. The fact that the water molecule prefers to form a hydrogen bond with O, despite there being two F adatoms adjacent to the Mo adsorption site, suggests that dissociation by releasing an H towards the O adatom is more likely. An additional hint of this preference can be found by comparing the positions of the atoms of the surface before and after water adsorption: while the surface oxygen atom moves 0.03 Å towards the water adsorption site, the two nearest fluorine move 0.82 Å away.

In its dissociation TS configuration, the water molecule is placed on a bridge site (centre images of Fig. 7). The H that was directed at the surface O now bridges the two oxygens, with a lengthened O-H bond length of 1.19 Å; the distance between this hydrogen and the surface O is now reduced to 1.25 Å. The calculated dissociation energy barrier is 0.14 eV, which is extraordinarily low for an MXene with a surface termination. After water dissociation, two OH groups are formed, and they remain adsorbed on the MXene on neighbouring hollow sites (right images of Fig. 7). The reaction activation energy found for this surface is lower than the ones calculated for most bare MXenes and is only surpassed by the bare MXenes made of metals of group 4 of the Periodic Table of the Elements [21]. There are several facts that can contribute to such an easy dissociation: (i) most of the nearby MXene termination is composed of F adatoms, which are easier to displace along the surface than O adatoms, so that (ii) water adsorption occurs via Mo-O bonding, and (iii) MXenes with surface termination containing hydroxyl groups are common, indicating that the system is stable if the O adatom becomes an OH group. The site where the two OH groups are adsorbed is not their most stable one (hollow-C). This can be advantageous for removing the products of water dissociation from the surface to regenerate the catalyst, and may increase the OH reactivity with other potential adsorbates if one wishes to catalyse more complex processes that begin with water dissociation. For example, if one intended to realize the WGSR, CO would need to adsorb near at least one of the OH, and we verified that it can indeed adsorb between the two OH left behind after water dissociation, on the only hollow site above an F adatom, with an adsorption energy around − 1.51 eV, as shown in Fig. S1 of the Supporting Information.

The mechanism of water adsorption and dissociation on our two-O Mo_2CT_x model, shown in Fig. 8, is analogous to the one found when only one O is present on the surface. The water molecule again adsorbs through the formation of an Mo-O bond with order 0.30 and length 2.38 Å (left images of Fig. 8). This bond is slightly longer, by 0.04 Å, than the corresponding one found for the one-O model, which makes sense given the fact that it is also of a slightly lower bond order, by 0.03,

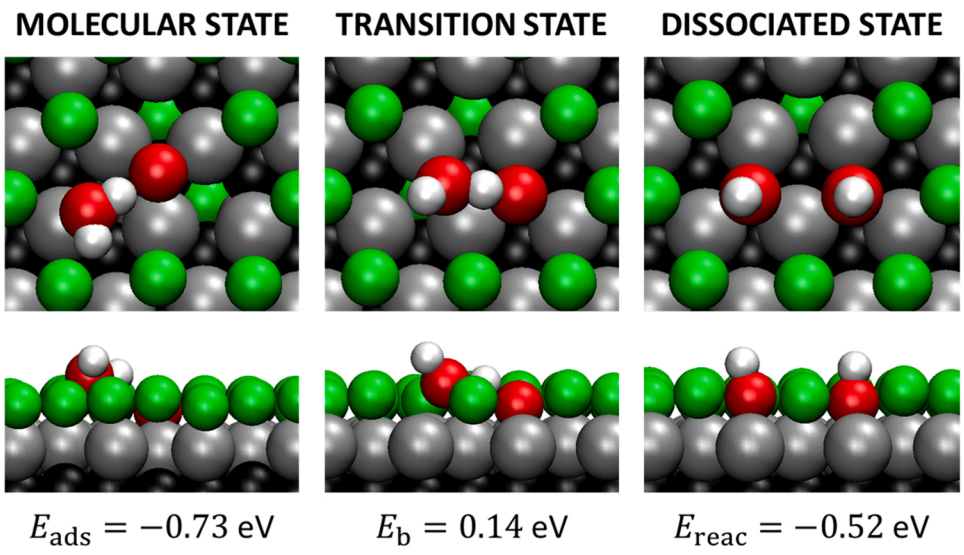

Fig. 7. Top (top images) and side (bottom images) views of the ground state configuration of a water molecule adsorbed on Mo_2CT_X (left images), the saddle point configuration of water dissociation (centre images), and the dissociated configuration (right images). The T_x surface termination is composed of F adatoms, except for a small region where an O adatom lies. The adsorption energy (E_{ads}), activation energy (E_b), and reaction energy (E_{reac}) are shown below the system representations and compiled in Table S1. Colour code for spheres: C in black, O in red, F in green, Mo in grey, and H in white.

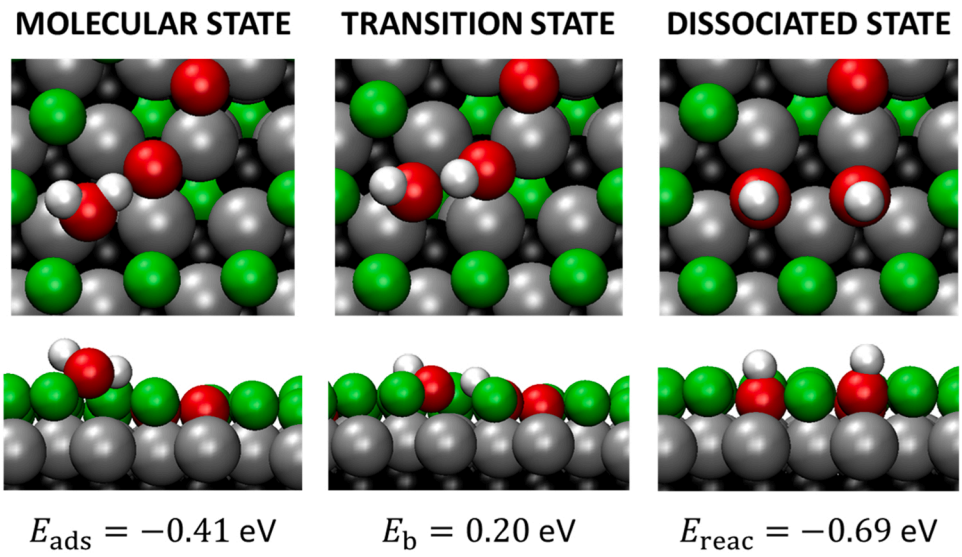

Fig. 8. Top (top images) and side (bottom images) views of the ground state configuration of a water molecule adsorbed on Mo_2CT_X (left images), the saddle point configuration of water dissociation (centre images), and the dissociated configuration (right images). The T_x surface termination is composed of F adatoms, except for a small region where two O adatoms lie. The adsorption energy (E_{ads}), activation energy (E_b), and reaction energy (E_{reac}) are shown below the system representations and compiled in Table S1. Colour code for spheres: C in black, O in red, F in green, Mo in grey, and H in white.

and that the adsorption is weaker, by 0.32 eV. The electron transfer is again directed towards the surface, but of only 0.07 *e*, and the O•••H hydrogen bond between the water H and the surface O has length 1.77 Å, which is shorter than the one predicted for the one-O Mo_2CT_x model by 0.05 Å. In the TS configuration for water dissociation, the water O atom is located at a bridge site (centre images of Fig. 8), and one of its O-H bonds is lengthened by 50 %, from 0.99 Å to 1.49 Å, as the H atom moves from the water O to one of the surface O. The calculated dissociation energy barrier is 0.20 eV, which is only 0.06 eV higher than on the one-O Mo_2CT_x model. The water dissociation reaction is more exothermic than on the one-O model, by 0.17 eV, and again results in the formation of two OH groups, adsorbed on neighbouring hollow sites of the MXene surface (right images of Fig. 8). For comparison with the one-O Mo_2CT_x model, we again studied CO adsorption in the vicinity of the OH groups. Instead of CO adsorbing on a hollow site and bonding to three Mo atoms, the repulsion from the extra surface O atom forces CO to adsorb on a top site and bond to only one Mo atom, as in Fig. S1. The adsorption energy becomes − 1.05 eV, which is about two thirds of the one calculated for the one-O model, but still fairly strong. One advantage of adsorbing on a top site instead of a hollow one is that the OC-OH distance is 2.66 Å, down from 2.83 Å, making it easier for these species to react with each other to form an OCOH intermediate [5,6].

4. Conclusions

In summary, we have studied the mechanism of the adsorption and dissociation of a water molecule, catalysed by the Mo_2CT_x MXene with an ABA atomic layer stacking, with different surface terminations. This reaction is crucial and often a rate-limiting step of reactions involved in the industrial production of hydrogen, such as steam reforming and the water gas shift reaction. This stacking was considered because our calculations showed that it is energetically more stable, and some of its structural parameters are closer to the ones experimentally measured for the Mo_2CT_x MXene with surface termination mostly composed by F and some O adatoms, on which the WGSR has been realized.

On the bare Mo_2C MXene surface, we found that water adsorbs moderately exothermically by forming an Mo-O covalent bond, and dissociates with an activation energy of 0.41 eV. The reaction is very exothermic by 1.38 eV. Bare patches of MXene surface are probably rare since this material easily oxidises but, if they do occur, they should provide active sites for catalysing water dissociation.

On both Mo_2CO_2 and Mo_2CF_2, i.e., the oxygen- and fluorine-terminated surfaces, we found that water adsorbs by forming very weak hydrogen bonds with the O and F surface atomic layers, respectively. This leads to a very high (2.50 eV) energy barrier for water dissociation on Mo_2CO_2, since O adatoms do not allow the molecule to form bonds with the Mo layer and change its dissociation mechanism. In contrast, on Mo_2CF_2, the F adatoms are not as tightly bound to their most favoured adsorption sites as O adatoms in Mo_2CO_2, and can move aside to allow water to form chemical bonds with Mo atoms, leading to a lower dissociation energy barrier of 0.31 eV. However, unlike what happens on Mo_2CO_2, the hydroxyl resulting from water dissociation strongly adsorbs on the surface, replacing the previously present F adatom, which is released in the form of HF. This is undesired, since it will contribute to the eventual replacement of all the F terminations by hydroxyl groups, hence damaging the catalytic surface.

The ideal region of the Mo_2CT_x MXene to serve as catalyst for water dissociation should simultaneously allow water to adsorb by bonding to the Mo layer, display an absolute adsorption energy greater than on Mo_2CF_2, and allow water to dissociate without the products of the reaction spontaneously removing atoms that should stay on the surface. To this end, (i) the MXene must have a surface termination, lest it become covered by an oxygen layer, (ii) the surface termination must not contain too much oxygen, as it becomes too inert and unsuited as a catalyst for water dissociation, and (iii) the surface cannot be fully terminated by fluorine, since the dissociation of water on Mo_2CF_2 results in the release of an HF molecule. Our calculations suggest that a region of the Mo_2CT_x MXene with surface termination composed of F adatoms, except for one or two O adatoms, satisfies all these requirements. We found that, on such regions, water adsorbs moderately exothermically (E_{ads} is −0.73 and −0.41 eV, respectively), by bonding to a surface Mo atom, dissociates with very low energy barriers of 0.14 and 0.20 eV, respectively, and the dissociation is moderately exothermic (E_{reac} is −0.52 and −0.69 eV, respectively). In addition, the products of the reaction (hydroxyl groups) remain adsorbed on the surface, but not immediately on their favourite adsorption site, which may facilitate their removal to regenerate the catalyst and/or increase their reactivity for subsequent steps of more complex processes beginning with water dissociation.

CRediT authorship contribution statement

José D. Gouveia: Conceptualization, Formal Analysis, Investigation, Writing - Original Draft, Visualization, **José R. B. Gomes**: Conceptualization, Resources, Writing - Review & Editing, Supervision, Project administration, Funding acquisition.

Declaration of Competing Interest

The authors declare that they have no known competing financial interests or personal relationships that could have appeared to influence the work reported in this paper.

Data availability

Data will be made available on request.

Acknowledgements

This work was developed within the scope of the project CICECO-Aveiro Institute of Materials, UIDB/50011/2020, UIDP/50011/2020 and LA/P/0006/2020, financed by national funds through the Fundação para a Ciência e a Tecnologia / Ministério da Educação e Ciência (FCT/MEC PIDDAC), Portugal. The authors are thankful to the National Network for Advanced Computing, Portugal, for additional computational resources granted through the project 2021.09799.CPCA.

Appendix A. Supporting information

Supplementary data associated with this article can be found in the online version at doi:10.1016/j.cattod.2022.07.016.

References

[1] L. Chen, Z. Qi, S. Zhang, J. Su, G.A. Somorjai, Catalytic hydrogen production from methane: a review on recent progress and prospect, Catalysts 10 (2020) 858, https://doi.org/10.3390/catal10080858.
[2] R.V. Afonso, J.D. Gouveia, J.R.B. Gomes, Catalytic reactions for H_2 production on multimetallic surfaces: a review, J. Phys.: Energy 3 (2021), 032016, https://doi.org/10.1088/2515-7655/ac0d9f.
[3] R. Morales-Salvador, J.D. Gouveia, Á. Morales-García, F. Viñes, J.R.B. Gomes, F. Illas, Carbon capture and usage by MXenes, ACS Catal. 11 (2021) 11248–11255, https://doi.org/10.1021/acscatal.1c02663.
[4] A. Otto, T. Grube, S. Schiebahn, D. Stolten, Closing the loop: captured CO_2 as a feedstock in the chemical industry, Energy Environ. Sci. 8 (2015) 3283–3297, https://doi.org/10.1039/C5EE02591E.
[5] A.A. Gokhale, J.A. Dumesic, M. Mavrikakis, On the mechanism of low-temperature water gas shift reaction on copper, J. Am. Chem. Soc. 130 (2008) 1402–1414, https://doi.org/10.1021/ja0768237.
[6] J.L.C. Fajín, M.N.D.S. Cordeiro, F. Illas, J.R.B. Gomes, Influence of step sites in the molecular mechanism of the water gas shift reaction catalyzed by copper, J. Catal. 268 (2009) 131–141, https://doi.org/10.1016/j.jcat.2009.09.011.
[7] M. Naguib, M. Kurtoglu, V. Presser, J. Lu, J. Niu, M. Heon, L. Hultman, Y. Gogotsi, M.W. Barsoum, Two-dimensional nanocrystals produced by exfoliation of Ti_3AlC_2, Adv. Mater. 23 (2011) 4248–4253, https://doi.org/10.1002/adma.201102306.
[8] M. Alhabeb, K. Maleski, T.S. Mathis, A. Sarycheva, C.B. Hatter, S. Uzun, A. Levitt, Y. Gogotsi, Selective etching of silicon from Ti_3SiC_2 (MAX) to obtain 2D titanium carbide (MXene), Angew. Chem. Int. Ed. 57 (2018) 5444–5448, https://doi.org/10.1002/anie.201802232.
[9] M. Naguib, Y. Gogotsi, Synthesis of two-dimensional materials by selective extraction, Acc. Chem. Res. 48 (2015) 128–135, https://doi.org/10.1021/ar500346b.
[10] J. Peng, X. Chen, W.J. Ong, X. Zhao, N. Li, Surface and heterointerface engineering of 2D MXenes and their nanocomposites: insights into electro- and photocatalysis, Chem 5 (2019) 18–50, https://doi.org/10.1016/j.chempr.2018.08.037.
[11] B. Anasori, M.R. Lukatskaya, Y. Gogotsi, 2D metal carbides and nitrides (MXenes) for energy storage, Nat. Rev. Mater. 2 (2017) 16098, https://doi.org/10.1038/natrevmats.2016.98.
[12] Á. Morales-García, F. Calle-Vallejo, F. Illas, MXenes: new horizons in catalysis, ACS Catal. 10 (2020) 13487–13503, https://doi.org/10.1021/acscatal.0c03106.
[13] P.O.Å. Persson, J. Rosen, Current state of the art on tailoring the MXene composition, structure, and surface chemistry, Curr. Opin. Solid State Mater. Sci. 23 (2019), 100774, https://doi.org/10.1016/j.cossms.2019.100774.
[14] E.B. Deeva, A. Kurlov, P.M. Abdala, D. Lebedev, S.M. Kim, C.P. Gordon, A. Tsoukalou, A. Fedorov, C.R. Müller, In situ XANES/XRD study of the structural stability of two-dimensional molybdenum carbide Mo_2CT_x: implications for the catalytic activity in the water–gas shift reaction, Chem. Mater. 31 (2019) 4505–4513, https://doi.org/10.1021/acs.chemmater.9b01105.
[15] J. Halim, K.M. Cook, M. Naguib, P. Eklund, Y. Gogotsi, J. Rosen, M.W. Barsoum, X-ray photoelectron spectroscopy of select multi-layered transition metal carbides (MXenes), Appl. Surf. Sci. 362 (2016) 406–417, https://doi.org/10.1016/j.apsusc.2015.11.089.
[16] J. Lu, I. Persson, H. Lind, J. Palisaitis, M. Li, Y. Li, K. Chen, J. Zhou, S. Du, Z. Chai, Z. Huang, L. Hultman, P. Eklund, J. Rosen, Q. Huang, P.O.Å. Persson, $Ti_{n+1}C_n$ MXenes with fully saturated and thermally stable Cl terminations, Nanoscale Adv. 1 (2019) 3680–3685, https://doi.org/10.1039/C9NA00324J.
[17] T. Wu, X. Pang, S. Zhao, S. Xu, Z. Liu, Y. Li, F. Huang, One-step construction of ordered sulfur-terminated tantalum carbide MXene for efficient overall water splitting, Small Struct. 3 (2022), 2100206, https://doi.org/10.1002/sstr.202100206.
[18] M. Peng, M. Dong, W. Wei, H. Xu, C. Liu, C. Shen, The introduction of amino termination on Ti_3C_2 MXene surface for its flexible film with excellent property, Carbon 179 (2021) 400–407, https://doi.org/10.1016/j.carbon.2021.04.049.
[19] J. Björk, J. Rosen, Functionalizing MXenes by tailoring surface terminations in different chemical environments, Chem. Mater. 33 (2021) 9108–9118, https://doi.org/10.1021/acs.chemmater.1c01264.
[20] J.D. Gouveia, F. Viñes, F. Illas, J.R.B. Gomes, MXenes atomic layer stacking phase transitions and their chemical activity consequences, Phys. Rev. Mater. 4 (2020), 054003, https://doi.org/10.1103/PhysRevMaterials.4.054003.
[21] J.D. Gouveia, Á. Morales-García, F. Viñes, F. Illas, J.R.B. Gomes, MXenes as promising catalysts for water dissociation, Appl. Catal. B: Environ. 260 (2020), 118191, https://doi.org/10.1016/j.apcatb.2019.118191.
[22] J.L. Hart, K. Hantanasirisakul, A.C. Lang, B. Anasori, D. Pinto, Y. Pivak, J.T. van Omme, S.J. May, Y. Gogotsi, M.L. Taheri, Control of MXenes' electronic properties through termination and intercalation, Nat. Commun. (2019), https://doi.org/10.1038/s41467-018-08169-8.
[23] J.D. Gouveia, G. Novell-Leruth, P.M.L.S. Reis, F. Viñes, F. Illas, J.R.B. Gomes, First-principles calculations on the adsorption behavior of amino acids on a titanium carbide MXene, ACS Appl. Bio Mater. 3 (2020) 5913–5921, https://doi.org/10.1021/acsabm.0c00621.
[24] A. Junkaew, R. Arróyave, Enhancement of the selectivity of MXenes (M_2C, M = Ti, V, Nb, Mo) via oxygen-functionalization: promising materials for gas-sensing and -separation, Phys. Chem. Chem. Phys. 20 (2018) 6073–6082, https://doi.org/10.1039/C7CP08622A.
[25] J.D. Gouveia, G. Novell-Leruth, F. Viñes, F. Illas, J.R.B. Gomes, The Ti_2CO_2 MXene as a nucleobase 2D sensor: a first-principles study, Appl. Surf. Sci. 544 (2021), 148946, https://doi.org/10.1016/j.apsusc.2021.148946.
[26] V. Parey, B.M. Abraham, M. v Jyothirmai, J.K. Singh, Mechanistic insights for electrochemical reduction of CO_2 into hydrocarbon fuels over O-terminated MXenes, Catal. Sci. Technol. (2022), https://doi.org/10.1039/D1CY02188E.
[27] Z. Li, Y. Cui, Z. Wu, C. Milligan, L. Zhou, G. Mitchell, B. Xu, E. Shi, J.T. Miller, F. H. Ribeiro, Y. Wu, Reactive metal–support interactions at moderate temperature in two-dimensional niobium-carbide-supported platinum catalysts, Nat. Catal. 1 (2018) 349–355, https://doi.org/10.1038/s41929-018-0067-8.
[28] G. Kresse, J. Hafner, Ab initio molecular dynamics for liquid metals, Phys. Rev. B 47 (1993) 558–561, https://doi.org/10.1103/PhysRevB.47.558.
[29] G. Kresse, J. Hafner, Ab initio molecular-dynamics simulation of the liquid-metal–amorphous-semiconductor transition in germanium, Phys. Rev. B 49 (1994) 14251–14269, https://doi.org/10.1103/PhysRevB.49.14251.
[30] G. Kresse, J. Furthmüller, Efficient iterative schemes for ab initio total-energy calculations using a plane-wave basis set, Phys. Rev. B 54 (1996) 11169–11186, https://doi.org/10.1103/PhysRevB.54.11169.
[31] G. Kresse, J. Furthmüller, Efficiency of ab-initio total energy calculations for metals and semiconductors using a plane-wave basis set, Comput. Mater. Sci. 6 (1996) 15–50, https://doi.org/10.1016/0927-0256(96)00008-0.
[32] J.P. Perdew, K. Burke, M. Ernzerhof, Generalized gradient approximation made simple, Phys. Rev. Lett. 77 (1996) 3865–3868, https://doi.org/10.1103/PhysRevLett.77.3865.
[33] S. Grimme, J. Antony, S. Ehrlich, H. Krieg, A consistent and accurate ab initio parametrization of density functional dispersion correction (DFT-D) for the 94 elements H-Pu, J. Chem. Phys. 132 (2010), 154104, https://doi.org/10.1063/1.3382344.
[34] S. Grimme, S. Ehrlich, L. Goerigk, Effect of the damping function in dispersion corrected density functional theory, J. Comput. Chem. 32 (2011) 1456–1465, https://doi.org/10.1002/jcc.21759.
[35] J.P.P. Ramalho, J.R.B. Gomes, F. Illas, Accounting for van der Waals interactions between adsorbates and surfaces in density functional theory based calculations: selected examples, RSC Adv. 3 (2013) 13085, https://doi.org/10.1039/c3ra40713f.
[36] F. Viñes, O. Lamiel-García, Approaching the quantitative description of enantioselective adsorption by the density functional theory means, J. Phys. Chem. C 123 (2019) 11714–11722, https://doi.org/10.1021/acs.jpcc.9b01463.
[37] J.D. Gouveia, Á. Morales-García, F. Viñes, J.R.B. Gomes, F. Illas, Facile heterogeneously catalyzed nitrogen fixation by MXenes, ACS Catal. 10 (2020) 5049–5056, https://doi.org/10.1021/acscatal.0c00935.
[38] Á. Morales-García, A. Fernández-Fernández, F. Viñes, F. Illas, CO_2 abatement using two-dimensional MXene carbides, J. Mater. Chem. A 6 (2018) 3381–3385, https://doi.org/10.1039/C7TA11379J.
[39] P.E. Blöchl, Projector augmented-wave method, Phys. Rev. B 50 (1994) 17953–17979, https://doi.org/10.1103/PhysRevB.50.17953.
[40] H.J. Monkhorst, J.D. Pack, Special points for Brillouin-zone integrations, Phys. Rev. B 13 (1976) 5188–5192, https://doi.org/10.1103/PhysRevB.13.5188.
[41] G. Henkelman, H. Jónsson, A dimer method for finding saddle points on high dimensional potential surfaces using only first derivatives, J. Chem. Phys. (1999), https://doi.org/10.1063/1.480097.
[42] W. Sun, Y. Li, B. Wang, X. Jiang, M.I. Katsnelson, P. Korzhavyi, O. Eriksson, I. di Marco, A new 2D monolayer BiXene, M_2C (M = Mo, Tc, Os), Nanoscale 8 (2016) 15753–15762, https://doi.org/10.1039/C6NR03602C.

[43] J.D. Gouveia, J.R.B. Gomes, Structural and energetic properties of vacancy defects in MXene surfaces, Phys. Rev. Mater. 6 (2022), 024004, https://doi.org/10.1103/PhysRevMaterials.6.024004.

[44] N. Zhang, Y. Hong, S. Yazdanparast, M. Asle Zaeem, Superior structural, elastic and electronic properties of 2D titanium nitride MXenes over carbide MXenes: a comprehensive first principles study, 2D Mater. 5 (2018), 045004, https://doi.org/10.1088/2053-1583/aacfb3.

[45] M. Naguib, V.N. Mochalin, M.W. Barsoum, Y. Gogotsi, 25th anniversary article: MXenes: a new family of two-dimensional materials, Adv. Mater. 26 (2014) 992–1005, https://doi.org/10.1002/adma.201304138.

[46] S. Bae, Y.-G. Kang, M. Khazaei, K. Ohno, Y.-H. Kim, M.J. Han, K.J. Chang, H. Raebiger, Electronic and magnetic properties of carbide MXenes – the role of electron correlations, Mater. Today Adv. 9 (2021), 100118, https://doi.org/10.1016/j.mtadv.2020.100118.

[47] T.A. Manz, Introducing DDEC6 atomic population analysis: part 3. Comprehensive method to compute bond orders, RSC Adv. 7 (2017) 45552–45581, https://doi.org/10.1039/C7RA07400J.